Int J Multiphase Flow Vol. 11, No. 5, pp. 699–712, 1985
Printed in Great Britain.

0801–9322/85 $3.00 + .00

SEDIMENTATION OF TWO ARBITRARILY ORIENTED SPHEROIDS IN A VISCOUS FLUID

SANGTAE KIM
Department of Chemical Engineering, University of Wisconsin, 1415 Johnson Drive, Madison, WI 53706, U.S.A.
and Mathematics Research Center, University of Wisconsin, 610 Walnut Street, Madison, WI 53705, U.S.A.

(*Received* 20 *February* 1984; *in revised form* 5 *June* 1984)

Abstract—The translational and rotational motions of two prolate spheroids sedimenting in a viscous fluid have been determined by the method of reflections. No restrictions are imposed on the spheroid orientations or relative sizes. As is the case in many mobility problems, the method converged rapidly for all but almost touching configurations. The results extend earlier work on special cases such as Wakiya's work on horizontal orientations and agree with Gluckman *et al.* and Liao and Krueger's boundary collocation solution of axisymmetric problems. Analysis of sedimentation with inclined axes and mirror symmetric geometry reveal both periodic and single-encounter particle trajectories. The calculation of the separatrix between the two behaviors required the use of the higher reflections introduced in this work.

1. INTRODUCTION

Suspensions of prolate spheroids have played an important role in the theoretical development of suspension rheology. Such suspensions exhibit non-Newtonian behavior through the interaction between the flow field and Brownian motion (Giesekus 1962, Brenner 1972, Hinch & Leal 1972). However, rigorous derivation of the material functions to date have been restricted to the dilute limit, partly because of the lack of information on multiparticle hydrodynamic interactions. Existing information on particle–particle interactions is limited to certain geometries at large particle–particle separations (Wakiya 1965) or special configurations (Gluckman *et al.* 1971; Liao & Krueger 1980).

New results are presented here which describe the interactions between two spheroids with arbitrary configurations and all but almost-touching separations. Explicit examples are worked out to illustrate phenomena, such as the evolution of particle geometry, which are not found in the corresponding problem for spheres. The computational technique which is based on the method of reflections (Happel & Brenner 1965, Felderhof 1977) was found to converge rapidly for the sedimentation and related mobility problems. The improved results for the mobility functions were essential in accurate calculation of particle trajectories, especially in the near-field interactions.

In section 2, the techniques for calculating hydrodynamic interactions which were developed in an earlier note (Kim 1985) are used to recover Wakiya's (1965) results for the resistance problem. In section 3, sedimentation and angular velocities are calculated to $O(R^{-7})$ and $O(R^{-8})$, respectively, where R is the center to center separation between the spheroids. An advantage of the present method is that it bypasses the usual procedure of calculation and inversion of the resistance problem. As outlined in Kim (1983), the sedimentation problem is solved directly, without solving a collection of subsidiary problems on translating and rotating spheroids. Problems solved include sedimentation along and perpendicular to the line of centers and the evolution of configurations for spheroids with inclined axes.

2. HYDRODYNAMIC INTERACTION BETWEEN TWO STATIONARY SPHEROIDS

In this section, the method will be used to recover Wakiya's (1965) calculations for the drag on a spheroid. Figure 1 shows the geometry used by Wakiya (1965). In order to simplify

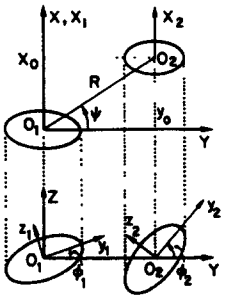

Figure 1. Wakiya's geometry for two horizontally oriented spheroids.

the final expressions, he restricted his analysis to two identical spheroids with both axes placed horizontally (with gravity acting in the negative z direction). The drag and torque on spheroid 1 was calculated for the case where both spheroids were translating (without rotating) in the negative x direction in a quiescent fluid.

In the terminology of the general literature, this is called a resistance problem. The translational and rotational velocities are specified and the drag and torques are to be found. The mobility problems pose the inverse question, i.e. forces and torques on the particle are specified and the translational and rotational motions are to be determined. The latter problem occurs more frequently in the modeling efforts of diverse fields. Sedimentation and diffusion problems in suspension rheology and hydrodynamic interactions in the Rouse & Zimm theory all require the solution of a mobility problem. Specific applications can be found in the following samples from an extensive list: Glendinning & Russel (1982), Batchelor (1976), and Bird, *et al.* (1977).

The sedimentation problem (a mobility problem) and the problem of calculating the drag on stationary objects (a resistance problem) are reciprocals of each other up to $O(R^{-3})$. This simple situation does not hold at higher orders because torques are present in the resistance but absent in the sedimentation problem. Torques, if present, contribute terms of $O(R^{-4})$ in the drag. Therefore, Wakiya's (1965) analysis of the drag to $O(R^{-2})$ also gives the sedimentation velocity to at least that order.

Wakiya's problem is equivalent to that of two stationary spheroids in a uniform stream with the stream flowing in the positive x direction (figure 1). We start by deriving the method of reflections solution to Wakiya's resistance problem, but without any simplifications regarding relative sizes, or spheroid orientations in the uniform stream $\mathbf{U}^\infty$. As in Wakiya's work, the analysis in this section will be carried out to two reflections so that the drag will be accurate to $O(R^{-2})$. The orientation vector, position along the axis, eccentricity and the distance from the centroid to the foci of each spheroid will be denoted by d_α, e_α and c_α, $\alpha = 1, 2$.

In an earlier note (Kim 1985) it was shown that the Chwang & Wu (1974, 1975) representation for the reflection from the uniform stream and the contribution from this (zeroth) reflection to the drag on spheroid 1 are

$$\mathbf{v}_1(\mathbf{x}) = \mathbf{U}^\infty - \mathbf{U}^\infty \cdot \{\alpha_1 \mathbf{d}_1\mathbf{d}_1 + \alpha_2(\delta - \mathbf{d}_1\mathbf{d}_1)\} \cdot \int_{-c_1}^{c_1} \left\{1 + (c_1^2 - \xi_1^2)\frac{(1 - e_1^2)}{(4e_1^2)}\nabla^2\right\} \mathbf{I}(\mathbf{x} - \xi_1)\mathrm{d}\xi_1, \qquad [2.1]$$

$$\mathbf{F}_1^{(0)} = 16\pi\mu c_1\{\alpha_1\mathbf{d}_1\mathbf{d}_1 + \alpha_2(\delta - \mathbf{d}_1\mathbf{d}_1)\} \cdot \mathbf{U}^\infty. \qquad [2.2]$$

The Chwang–Wu constants α and γ depend only on the spheroid eccentricities and are given in table 1 and $\mathbf{I}$ is the Oseen tensor. The analogous reflection field $\mathbf{v}_2$ from spheroid 2 can be obtained from [2.1] by permuting the particle indices. As shown in the references on the

Table 1. Constants for the velocity representation for the spheroid Constants derived from Chwang & Wu (1974, 1975)

$$\alpha_1 = e^2\left\{-2e + (1+e^2)\log\left(\frac{1+e}{1-e}\right)\right\}^{-1}$$

$$\alpha_2 = 2e^2\left\{2e + (3e^2-1)\log\left(\frac{1+e}{1-e}\right)\right\}^{-1}$$

$$\gamma = (1-e^2)\left\{2e - (1-e^2)\log\left(\frac{1+e}{1-e}\right)\right\}^{-1}$$

$$\gamma_3 = (1-e^2)\left\{-2e + (1+e^2)\log\left(\frac{1+e}{1-e}\right)\right\}^{-1}$$

$$\gamma_3' = \gamma_3(1-e^2)^{-1}$$

$$\alpha_3 = 2e^2\gamma_3\left\{-2e + \log\left(\frac{1+e}{1-e}\right)\right\}\left\{2e(2e^2-3) + 3(1-e^2)\log\left(\frac{1+e}{1-e}\right)\right\}^{-1}$$

$$\alpha_3' = e^2\gamma_3'\left\{-2e + (1-e^2)\log\left(\frac{1+e}{1-e}\right)\right\}\left\{2e(2e^2-3) + 3(1-e^2)\log\left(\frac{1+e}{1-e}\right)\right\}^{-1}$$

$$\alpha_4 = 2e^2(1-e^2)\left\{2e(3-5e^2) - 3(1-e^2)^2\log\left(\frac{1+e}{1-e}\right)\right\}^{-1}$$

$$\alpha_5 = e^2\left\{6e - (3-e^2)\log\left(\frac{1+e}{1-e}\right)\right\}^{-1}$$

$$\alpha' = \alpha_3 + \alpha_3' = e^2\left\{-2e + (1+e^2)\log\left(\frac{1+e}{1-e}\right)\right\}^{-1}$$

$$\gamma' = \gamma_3 + \gamma_3' = (2-e^2)\left\{-2e + (1+e^2)\log\left(\frac{1+e}{1-e}\right)\right\}^{-1}$$

$$\alpha^* = \alpha_3 - \alpha_3'$$

$$\gamma^* = \gamma_3 - \gamma_3' = -e^2\left\{-2e + (1+e^2)\log\left(\frac{1+e}{1-e}\right)\right\}^{-1}$$

method of reflections, this implies that the contribution from the first reflection is

$$\begin{aligned}\mathbf{F}_1^{(1)} &= 8\pi\mu\{\alpha_1\mathbf{d}_1\mathbf{d}_1 + \alpha_2(\delta - \mathbf{d}_1\mathbf{d}_1)\} \\ &\quad \cdot \int_{-c_1}^{c_1}\left\{1 + (c_1^2 - \xi_1^2)\frac{(1-e_1^2)}{(4e_1^2)}\nabla^2\right\}\mathbf{v}_2(\xi_1)\mathrm{d}\xi_1 \\ &= -16\pi\mu c_1\{\alpha_1\mathbf{d}_1\mathbf{d}_1 + \alpha_2(\delta - \mathbf{d}_1\mathbf{d}_1)\} \cdot \int_{-c_1}^{c_1}\frac{\mathrm{d}\xi_1}{2c_1}\int_{-c_2}^{c_2}\frac{\mathrm{d}\xi_2}{2c_2} \\ &\quad \cdot\left[1 + \left((c_1^2 - \xi_1^2)\frac{(1-e_1^2)}{(4e_1^2)} + (c_2^2 - \xi_2^2)\frac{(1-e_2^2)}{(4e_2^2)}\right)\nabla^2\right] \\ &\quad \mathbf{I}(\xi_1 - \xi_2)/(8\pi\mu) \cdot \mathbf{F}_2^{(0)}.\end{aligned} \tag{2.3}$$

It is apparent that the dependence on the orientation and shape of spheroids 1 and 2 comes solely from the tensor

$$\begin{aligned}\mathbf{T}_{12}^R &= \frac{8}{3}e\{\alpha_1\mathbf{d}_1\mathbf{d}_1 + \alpha_2(\delta - \mathbf{d}_1\mathbf{d}_1)\} \\ &\quad \cdot \int_{-c_1}^{c_1}\frac{\mathrm{d}\xi_1}{2c_1}\int_{-c_2}^{c_2}\frac{\mathrm{d}\xi_2}{2c_2}\left[1 + \left((c_1^2 - \xi_1^2)\frac{(1-e_1^2)}{(4e_1^2)}\right.\right. \\ &\quad \left.\left. + (c_2^2 - \xi_2^2)\frac{(1-e_2^2)}{(4e_2^2)}\right)\nabla^2\right]\mathbf{I}(\xi_1 - \xi_2)/(8\pi\mu).\end{aligned} \tag{2.4}$$

For the spherical case, this tensor is known to polymer kineticists as the Rotne–Prager–Yamakawa tensor (Rotne & Prager 1969, Yamakawa 1970). It is interesting to note that Rotne & Prager obtained their tensor using a variational approach.

The leading order term in the contribution from the second reflection,

$$\mathbf{F}_1^{(2)} = (-6\pi\mu a_1 \mathsf{T}_{12}^R) \cdot (-6\pi\mu a_2 \mathsf{T}_{21}^R) \cdot \mathbf{F}_1^{(0)},$$

comes from the monopole approximation

$$\mathsf{T}_{12}^R \sim \frac{8}{3} e\{\alpha_1 \mathbf{d}_1\mathbf{d}_1 + \alpha_2(\delta - \mathbf{d}_1\mathbf{d}_1)\} \cdot \mathsf{I}(\mathbf{x}_1 - \mathbf{x}_2)/(8\pi\mu). \qquad [2.5]$$

The drag on spheroid 1 is the sum of these contributions and Wakiya's (1965) solution is recovered after the appropriate simplifications in the geometry and notational changes. The contribution from the first reflection to $O(R^{-2})$ is simply a monopole–monopole interaction:

$$-2c_1\{\alpha_1 \mathbf{d}_1\mathbf{d}_1 + \alpha_2(\delta - \mathbf{d}_1\mathbf{d}_1)\} \cdot \mathsf{I}(\mathbf{x}_1 - \mathbf{x}_2) \cdot \mathbf{F}_2^{(0)}. \qquad [2.6]$$

To convert this into Wakiya's expression, we need

$$\mathbf{F}_2^{(0)} = 16\pi\mu c_2\{\alpha_1 \mathbf{d}_2\mathbf{d}_2 + \alpha_2(\delta - \mathbf{d}_2\mathbf{d}_2)\} \cdot \mathbf{U}^\infty, \qquad [2.6a]$$

$$\mathbf{U}^\infty \cdot (\mathbf{x}_2 - \mathbf{x}_1) = U^\infty R \sin\psi, \qquad [2.6b]$$

$$\mathbf{d}_1 \cdot \mathbf{U}^\infty = \mathbf{d}_2 \cdot \mathbf{U}^\infty = 0, \qquad [2.6c]$$

and $c_1 = c_2 = c$, $e_1 = e_2 = e$. Equation [2.6] can then be simplified to

$$-32\pi\mu(c\alpha_2)^2\mathbf{U}^\infty/R - 32\pi\mu c\alpha_2 U^\infty \sin\psi/R\{c\alpha_1 \mathbf{d}_1\mathbf{d}_1 + c\alpha_2(\delta - \mathbf{d}_1\mathbf{d}_1)\} \cdot (\mathbf{x}_2 - \mathbf{x}_1)/R. \qquad [2.7]$$

Therefore, the components of the drag in the direction of the uniform stream, spheroid axis and the third orthogonal axis (or x_1, y_1, z_1 in Wakiya's right handed coordinate system centered at $\mathbf{x}_1$) are

$$-32\pi\mu(c\alpha_2)^2 U^\infty(1 + \sin^2\psi)/R, \qquad [2.8a]$$

$$-32\pi\mu(c\alpha_1)(c\alpha_2)U^\infty \cos\phi_1 \sin\psi\cos\psi/R, \qquad [2.8b]$$

and

$$32\pi\mu(c\alpha_2)^2\mathbf{U}^\infty \sin\phi_1 \sin^2\psi\cos\psi/R. \qquad [2.8c]$$

Since $c\alpha_1$ and $c\alpha_2$ equal Wakiya's R_2 and R_1, respectively, we recover his $O(R^{-1})$ term.

The $O(R^{-2})$ terms come from the monopole–monopole interactions in the second reflection or

$$4c^2\{\alpha_1 \mathbf{d}_1\mathbf{d}_1 + \alpha_2(\delta - \mathbf{d}_1\mathbf{d}_1)\} \cdot \mathsf{I}(\mathbf{x}_1 - \mathbf{x}_2) \cdot \{\alpha_1 \mathbf{d}_2\mathbf{d}_2 + \alpha_2(\delta - \mathbf{d}_2\mathbf{d}_2)\} \cdot \mathsf{I}(\mathbf{x}_1 - \mathbf{x}_2) \cdot \mathbf{F}_1^{(0)}.$$

Some heavy algebra can be bypassed by noting that the leftmost tensor is the one that determines the direction of the drag. The product of the four factors to its right simplifies

to

$$16\pi\mu c_1\alpha_2^2/R^2\,\mathbf{U}^\infty - 16\pi\mu c_1\alpha_2^2 U^\infty \sin\psi/R^2\{\alpha_2(2+\sin^2\psi) + (\alpha_2\sin^2\phi_2 + \alpha_1\cos^2\phi_2)\cos^2\psi\}(\mathbf{x}_1-\mathbf{x}_2)/R + 16\pi\mu c_1\alpha_2^2(\alpha_1-\alpha_2)U^\infty\sin\psi\cos\psi\cos\phi_2/R^2\,\mathbf{d}_2$$

and the x_1, y_1, z_1 components reduce to the corresponding terms in Wakiya's [3.8].

The original expressions for the torque can also be recovered via the following contributions from the first and second reflections:

$$\mathbf{T}_1^{(1)} = 4\pi\mu\{\gamma\mathbf{d}_1\mathbf{d}_1 + \gamma'(\delta-\mathbf{d}_1\mathbf{d}_1)\}\cdot\int_{-c_1}^{c_1}(c_1^2-\xi_1^2)\nabla\times\mathbf{v}_2(\xi_1)d\xi_1 + 8\pi\mu\alpha'\mathbf{d}_1\times\int_{-c_1}^{c_1}(c_1^2-\xi_1^2)\{1+(c_1^2-\xi_1^2)\frac{(1-e_1^2)}{(8e_1^2)}\nabla^2\}\mathbf{d}_1\cdot\mathbf{e}_2(\xi_1)d\xi_1,$$

$$\mathbf{T}_1^{(2)} = 4\pi\mu\{\gamma\mathbf{d}_1\mathbf{d}_1 + \gamma'(\delta-\mathbf{d}_1\mathbf{d}_1)\}\cdot\int_{-c_1}^{c_1}(c_1^2-\xi_1^2)\nabla\times\mathbf{v}_{12}(\xi_1)d\xi_1 + 8\pi\mu\alpha'\mathbf{d}_1\times\int_{-c_1}^{c_1}(c_1^2-\xi_1^2)\{1+(c_1^2-\xi_1^2)\frac{(1-e_1^2)}{(8e_1^2)}\nabla^2\}\mathbf{d}_1\cdot\mathbf{e}_{12}(\xi_1)d\xi_1.$$

In the next section, the analogous expressions for the sedimentation (mobility) problem are calculated to higher order. From here on, we will not use the angles ϕ_1, ϕ_2 and ψ. Instead, the geometrical dependence will be represented by dot products between $\mathbf{x}_1-\mathbf{x}_2$, $\mathbf{d}_1$ and $\mathbf{d}_2$.

3. SEDIMENTATION OF TWO SPHEROIDS

3.1. *General procedure*

The procedure for calculating the sedimentation velocities is a straightforward generalization of that employed for spheres. The essential modification is the distribution of the singularities along the axes of the spheroids. The calculations will be performed up to and including the second reflection so that the error in the translational and rotational velocities will be $O(R^{-7})$ and $O(R^{-8})$, respectively.

The translational velocity of spheroid 1 is obtained by summing the contribution from the reflections:

$$\mathbf{U}_1 = \mathbf{U}_1^{(0)} + \mathbf{U}_1^{(1)} + \mathbf{U}_1^{(2)} + \cdots. \tag{3.1}$$

The zeroth reflection contributes

$$\mathbf{U}_1^{(0)} = \mathbf{F}_1(16\pi\mu c_1)^{-1}\cdot\{\alpha_1^{-1}\mathbf{d}_1\mathbf{d}_1 + \alpha_2^{-1}(\delta-\mathbf{d}_1\mathbf{d}_1)\}. \tag{3.2}$$

The contribution from the first reflection is

$$\mathbf{U}_1^{(1)} = \frac{1}{2c_1}\int_{-c_1}^{c_1}\left\{1+(c_1^2-\xi_1^2)\frac{(1-e_1^2)}{(4e_1^2)}\nabla^2\right\}\mathbf{v}_2(\xi_1)d\xi_1, \tag{3.3}$$

with the incident field

$$\mathbf{v}_2(\mathbf{x}) = \mathbf{F}_2\cdot\int_{-c_2}^{c_2}\left\{1+(c_2^2-\xi_2^2)\frac{(1-e_2^2)}{(4e_2^2)}\nabla^2\right\}\mathbf{I}(\mathbf{x}-\xi_2)/(16\pi\mu c_2)d\xi_2. \tag{3.4}$$

This contribution can be simplified as follows:

$$\begin{aligned}\mathbf{U}_1^{(1)} &= \mathbf{F}_2 \cdot \int_{-c_1}^{c_1} \frac{d\xi_1}{2c_1} \int_{-c_2}^{c_2} \frac{d\xi_2}{2c_2} \left[1 + \left((c_1^2 - \xi_1^2)\frac{(1-e_1^2)}{(4e_1^2)} \right.\right. \\ &\quad \left.\left. + (c_2^2 - \xi_2^2)\frac{(1-e_2^2)}{(4e_2^2)}\right)\nabla^2\right] \mathbf{I}(\xi_1 - \xi_2)/(8\pi\mu) \\ &= \frac{1}{8\pi\mu}\int_{-c_1}^{c_1} \frac{d\xi_1}{2c_1}\int_{-c_2}^{c_2}\frac{d\xi_2}{2c_2}\left\{\left[\frac{1}{\xi}\right.\right. \\ &\quad + \left((c_1^2 - \xi_1^2)\frac{(1-e_1^2)}{(4e_1^2)} + (c_2^2 - \xi_2^2)\frac{(1-e_2^2)}{(4e_2^2)}\right)\frac{2}{\xi^3}\Bigg]\mathbf{F}_2 \\ &\quad + \left[\frac{1}{\xi^3} - \left((c_1^2 - \xi_1^2)\frac{(1-e_1^2)}{(4e_1^2)}\right.\right. \\ &\quad \left.\left.\left. + (c_2^2 - \xi_2^2)\frac{(1-e_2^2)}{(4e_2^2)}\right)\frac{6}{\xi^5}\right]\boldsymbol{\xi}_{12}\boldsymbol{\xi}_{12}\cdot\mathbf{F}_2\right\},\end{aligned} \tag{3.5}$$

with $\boldsymbol{\xi}_{12} = \boldsymbol{\xi}_1 - \boldsymbol{\xi}_2$ and $\xi = |\boldsymbol{\xi}_{12}|$.

The second reflection contributes

$$\mathbf{U}_1^{(2)} = \frac{1}{2c_1}\int_{-c_1}^{c_1}\left\{1 + (c_1^2 - \xi_1^2)\frac{(1-e_1^2)}{(4e_1^2)}\nabla^2\right\}\mathbf{v}_{12}(\xi_1)d\xi_1, \tag{3.6}$$

with

$$\mathbf{v}_{12}(\mathbf{x}) = \mathbf{S}_2^{(1)} : \frac{3}{4c_2^3}\int_{-c_2}^{c_2}(c_2^2 - \xi_2^2)\left\{1 + (c_2^2 - \xi_2^2)\frac{(1-e_2^2)}{(8e_2^2)}\nabla^2\right\}\nabla\,\mathbf{I}(\mathbf{x} - \xi_2)/(8\pi\mu)d\xi_2. \tag{3.7}$$

When we insert [3.7] into [3.6] and use the expressions for the Stokes dipole and octupole, [3.6] simplifies to

$$\begin{aligned}&\frac{1}{8\pi\mu}\int_{-c_1}^{c_1}\frac{d\xi_1}{2c_1}\int_{-c_2}^{c_2}\frac{3\,d\xi_2}{4c_2^3}(c_2^2 - \xi_2^2) \\ &\quad\times\left\{\left[-\frac{3}{\xi^5} + \left((c_1^2 - \xi_1^2)\frac{(1-e_1^2)}{(4e_1^2)} + (c_2^2 - \xi_2^2)\frac{(1-e_2^2)}{(8e_2^2)}\right)\frac{30}{\xi^7}\right]\boldsymbol{\xi}_{12}\boldsymbol{\xi}_{12}\boldsymbol{\xi}_{12} : \mathbf{S}_2^{(1)}\right. \\ &\qquad\left. - \left[(c_1^2 - \xi_1^2)\frac{(1-e_1^2)}{(4e_1^2)} + (c_2^2 - \xi_2^2)\frac{(1-e_2^2)}{(8e_2^2)}\right]\frac{12}{\xi^5}\mathbf{S}_2^{(1)}\cdot\boldsymbol{\xi}_{12}\right\}.\end{aligned} \tag{3.8}$$

The stresslet is obtained via the Faxen law as (Kim 1985)

$$\begin{aligned}S_{2ij}^{(1)} &= 8\pi\mu\{-\tfrac{1}{2}\alpha_5(d_{2i}d_{2j} - \tfrac{1}{3}\delta_{ij})(d_{2k}d_{2l} - \tfrac{1}{3}\delta_{kl}) \\ &\quad - \tfrac{1}{4}\alpha^*(d_{2i}\delta_{jk}d_{2l} + d_{2i}\delta_{jl}d_{2k} + \delta_{il}d_{2j}d_{2k} + \delta_{ik}d_{2j}d_{2l} - 4d_{2i}d_{2j}d_{2k}d_{2l}) \\ &\quad - \tfrac{1}{2}\alpha_4(\delta_{ik}\delta_{jl} + \delta_{il}\delta_{jk} + \delta_{ij}d_{2k}d_{2l} + d_{2i}d_{2j}d_{2k}d_{2l} \\ &\quad - d_{2i}\delta_{jk}d_{2l} - d_{2i}\delta_{jl}d_{2k} - \delta_{il}d_{2j}d_{2k} - \delta_{ik}d_{2j}d_{2l})\} \\ &\quad\times\int_{-c_2}^{c_2}(c_2^2 - \xi_2^2)\left\{1 + (c_2^2 - \xi_2^2)\frac{(1-e_2^2)}{(8e_2^2)}\nabla^2\right\}e_{1kl}(\xi_2)d\xi_2 \\ &\quad - 2\pi\mu\gamma^*(d_{2i}\epsilon_{jkl}d_{2l} + d_{2j}\epsilon_{ikl}d_{2l})\int_{-c_2}^{c_2}(c_2^2 - \xi_2^2)\nabla\times\mathbf{v}_1(\xi_2)_k - 2\omega_2^{(1)}k\}d\xi_2.\end{aligned} \tag{3.9}$$

The expression for $\mathbf{U}_1^{(1)}$ is exact since the exact $\mathbf{v}_2$ is used while $\mathbf{U}_1^{(2)}$ is accurate only to $O(R^{-6})$ since only those leading terms were used in [3.7]. However, the leading error term, of $O(R^{-7})$, comes from the third reflection which was neglected.

The rotational velocity of spheroid 1 also follows as a sum of the contribution from each reflection:

$$\boldsymbol{\omega}_1 = \boldsymbol{\omega}_1^{(1)} + \boldsymbol{\omega}_1^{(2)} + \cdots . \tag{3.10}$$

The first reflection contributes

$$\begin{aligned}\boldsymbol{\omega}_1^{(1)} = {} & \frac{3}{8c_1^3}\int_{-c_1}^{c_1}(c_1^2-\xi_1^2)\nabla\times\mathbf{v}_2(\xi_1)\mathrm{d}\xi_1 \\ & + \frac{3}{4c_1^3}\frac{e_1^2}{(2-e_1^2)}\int_{-c_1}^{c_1}(c_1^2-\xi_1^2)\left\{1+(c_1^2-\xi_1^2)\right. \\ & \left.\cdot\frac{(1-e_1^2)}{(8e_1^2)}\nabla^2\right\}\mathbf{d}_1\times[\mathbf{e}_2(\xi_1)\cdot\mathbf{d}_1]\mathrm{d}\xi_1 .\end{aligned} \tag{3.11}$$

Substitutions for $\mathbf{v}_2$, its rate-of-strain field $\mathbf{e}_2$ and the expression for the rotlet eventually lead to

$$\begin{aligned}\boldsymbol{\omega}_1^{(1)} = {} & \frac{1}{8\pi\mu}\int_{-c_1}^{c_1}\frac{3}{4c_1^3}\mathrm{d}\xi_1\int_{-c_2}^{c_2}\frac{\mathrm{d}\xi_2}{2c_2}(c_1^2-\xi_1^2)\mathbf{F}_2\times\boldsymbol{\xi}_{12}/\xi^3 \\ & + \frac{1}{8\pi\mu}\frac{e_1^2}{(2-e_1^2)}\int_{-c_1}^{c_1}\frac{3\,\mathrm{d}\xi_1}{4c_1^3}\int_{-c_2}^{c_2}\frac{\mathrm{d}\xi_2}{2c_2}(c_1^2-\xi_1^2) \\ & \times\left\{\left[-\frac{3}{\xi^5}+\left((c_1^2-\xi_1^2)\frac{(1-e_1^2)}{(8e_1^2)}+(c_2^2-\xi_2^2)\right.\right.\right. \\ & \left.\left.\left.\cdot\frac{(1-e_2^2)}{(4e_2^2)}\right)\frac{30}{\xi^7}\right]\mathbf{F}_2\cdot\boldsymbol{\xi}_{12}\mathbf{d}_1\cdot\boldsymbol{\xi}_{12}\mathbf{d}_1\times\boldsymbol{\xi}_{12} \\ & - \left[(c_1^2-\xi_1^2)\frac{(1-e_1^2)}{(8e_1^2)}+(c_2^2-\xi_2^2)\right. \\ & \left.\cdot\frac{(1-e_2^2)}{(4e_2^2)}\right]\frac{6}{\xi^5}\mathbf{d}_1\times(\mathbf{F}_2\boldsymbol{\xi}_{12}+\boldsymbol{\xi}_{12}\mathbf{F}_2)\cdot\mathbf{d}_1\Big\} .\end{aligned} \tag{3.12}$$

The second reflection contributes

$$\begin{aligned}\boldsymbol{\omega}_1^{(2)} = {} & \frac{3}{8c_1^3}\int_{-c_1}^{c_1}(c_1^2-\xi_1^2)\nabla\times\mathbf{v}_{12}(\xi_1)\mathrm{d}\xi_1 \\ & + \frac{3}{4c_1^3}\frac{e_1^2}{(2-e_1^2)}\int_{-c_1}^{c_1}(c_1^2-\xi_1^2)\left\{1+(c_1^2-\xi_1^2)\right. \\ & \left.\cdot\frac{(1-e_1^2)}{(8e_1^2)}\nabla^2\right\}\mathbf{d}_1\times[\mathbf{e}_{12}(\xi_1)\cdot\mathbf{d}_1]\mathrm{d}\xi_1 .\end{aligned} \tag{3.13}$$

The leading order term in $\mathbf{v}_{12}$ is irrotational. Therefore, the $O(R^{-5})$ term in the rotational velocity comes solely from the second term in [3.13]. It should be noted that this term is absent for spheres, so for spheres, $\boldsymbol{\omega}_1^{(2)}$ decays more rapidly, i.e. as $O(R^{-7})$ [see Jeffrey &

Onishi (1984)]. Finally, [3.13] can be reduced to

$$\frac{1}{8\pi\mu}\frac{e_1^2}{(2-e_1^2)}\int_{-c_1}^{c_1}\frac{3\,d\xi_1}{4c_1^3}\int_{-c_2}^{c_2}\frac{3\,d\xi_2}{4c_2^3}(c_1^2-\xi_1^2)(c_2^2-\xi_2^2)$$
$$\times\left\{\left[-\frac{3}{\xi^5}+\left((c_1^2-\xi_1^2)\frac{(1-e_1^2)}{(8e_1^2)}+(c_2^2-\xi_2^2)\cdot\frac{(1-e_2^2)}{(8e_2^2)}\right)\frac{60}{\xi^7}\right]\mathbf{d}_1\cdot\boldsymbol{\xi}_{12}\mathbf{d}_1\times[\mathbf{S}_2^{(1)}\cdot\boldsymbol{\xi}_{12}]\right.$$
$$+\left[-\frac{3}{\xi^5}+\left((c_1^2-\xi_1^2)\frac{(1-e_1^2)}{(8e_1^2)}+(c_2^2-\xi_2^2)\cdot\frac{(1-e_2^2)}{(8e_2^2)}\right)\frac{60}{\xi^7}\right][\mathbf{S}_2^{(1)}:\boldsymbol{\xi}_{12}\mathbf{d}_1]\mathbf{d}_1\times\boldsymbol{\xi}_{12} \qquad [3.14]$$
$$-\left[(c_1^2-\xi_1^2)\frac{(1-e_1^2)}{(8e_1^2)}+(c_2^2-\xi_2^2)\frac{(1-e_2^2)}{(8e_2^2)}\right]\frac{12}{\xi^5}\mathbf{d}_1\times[\mathbf{S}_2^{(1)}\cdot\mathbf{d}_1]$$
$$+\left[\frac{15}{\xi^7}-\left((c_1^2-\xi_1^2)\frac{(1-e_1^2)}{(8e_1^2)}+(c_2^2-\xi_2^2)\cdot\frac{(1-e_2^2)}{(8e_2^2)}\right)\frac{210}{\xi^9}\right][\mathbf{S}_2^{(1)}:\boldsymbol{\xi}_{12}\boldsymbol{\xi}_{12}]\boldsymbol{\xi}_{12}\cdot\mathbf{d}_1\mathbf{d}_1\times\boldsymbol{\xi}_{12}\Bigg\}.$$

Equations [3.2], [3.5], [3.8], [3.9], [3.12], and [3.14] allow us to calculate the translational and rotational velocities for any given orientations of the spheroids. Special orientations are examined in the following subsections.

3.2. *Sedimentation of two vertically oriented spheroids along their line of centers*

The simplest geometry consists of two vertically oriented spheroids falling along their line of centers as shown in figure 2. The orientation and separation between the spheroids remain invariant as can be deduced from symmetry and the linearity of the Stokes equation. Thus the analysis leads to a straightforward extension of Stimson & Jeffery's (1926) results for spheres. Therefore this problem merely serves as a benchmark test for computational methods.

The sedimentation velocity, nondimensionalized by the terminal velocity for an isolated, vertically oriented spheroid, is plotted in figure 3 for three aspect ratios. The solid line is indistinguishable from the spherical (Stimson & Jeffery) solution for $R/a > 2.1$. As the aspect ratio increases, the hydrodynamic interactions become weaker. The contribution from reflections beyond those calculated by Wakiya become significant for $R/a < 3$. The results

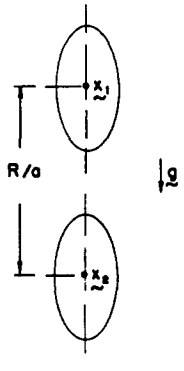

Figure 2. Sedimentation of two identical spheroids falling along their line of centers

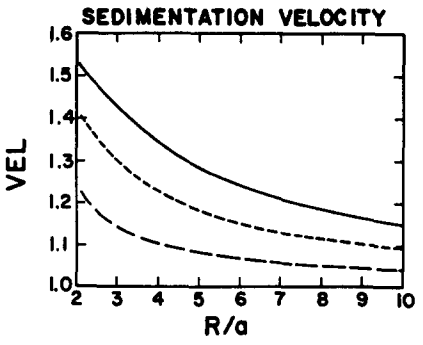

Figure 3. Sedimentation velocity versus center-to-center separtion for two spheroids as in figure 2. Aspect ratio of 1.01, —; aspect ratio of 2, - - -; aspect ratio of 10, – –.

also agree with those obtained by Gluckman *et al.* (1971) and Liao & Krueger (1980) as shown in table 2 of the appendix. Their λ factor, the drag nondimensionalized by the Stokes drag of the sphere with the same cross-sectional area, has been successfully reproduced.

3.3. *Sedimentation of two horizontally oriented spheroids*

The analysis of two spheres falling perpendicular to their line of centers can be extended to the spheroidal case (figure 4). However, to keep the geometry invariant, the spheroid axes must be perpendicular to both gravity and the line of centers.

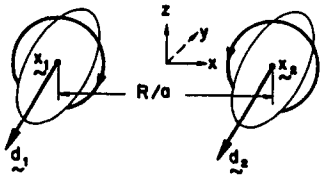

Figure 4. Sedimentation of two horizontally and parallely oriented spheroids.

Figures 5 and 6 show the sedimentation and angular velocities for the same aspect ratios as before. The terminal velocity of an isolated, horizontally oriented spheroid was used to scale both $-U_z$ and $-\omega_y a$. In both figures the solid line is indistinguishable from the result for spheres (Goldman, *et al.* 1966). The dependence on the aspect ratio is qualitatively similar to that found in the previous subsection. Finally, it should be noted that for the geometry considered in this subsection, the $O(R^{-5})$ term vanishes in [3.13] for the rotational velocity.

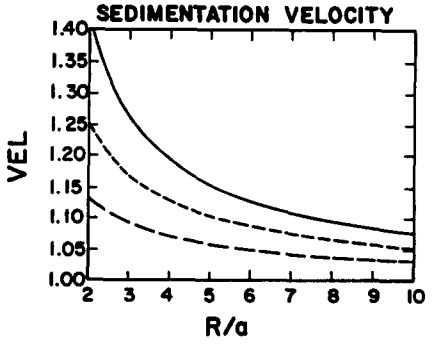

Figure 5. Sedimentation velocity versus center-to-center separation for two spheroids as in figure 4. Aspect ratio of 1.01, —; aspect ratio of 2, - - -; aspect ratio of 10, – –.

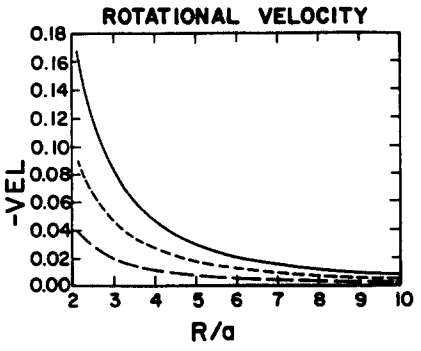

Figure 6. Angular velocity versus center-to-center separation for two spheroids as in figure 4. Aspect ratio of 1.01, —; aspect ratio of 2, - - -; aspect ratio of 10, – –.

3.4. *Sedimentation of two inclined spheroids*

The results in the preceding subsections were qualitatively similar to that found for spheres, and were mainly of interest as benchmarks for the computational technique. Here, we turn our attention to a situation where the results differ qualitatively because of the evolution of the particle geometry. Figure 7 shows two inclined spheroids settling with their axes lying in a common vertical plane. Mirror symmetry has been introduced to reduce the number of parameters, but the algorithm from subsection 3.1 can handle more general situations. At all times, the geometry is specified by the dimensionless center-to-center separation, R/a and θ, the polar angle for $\mathbf{d}_1$.

The successive improvement obtained with each new reflection is shown in table 1 of the appendix. At all but small separations, our two-reflection solution provides accurate answers. For spheres the exact result is available (Goldman *et al.* 1966) and we see that even at fairly small separations, the relative error is under 10% because of the small contributions from the neglected terms.

The evolution of the geometry is caused by the anisotropy in the mobility tensors and the rotation of the spheroids about their respective minor axes. Since the mobility is greater in the axial than in the transverse direction, an inclined spheroid drifts horizontally as it settles. At the same time, the spheroid rotation changes the orientation of the axis. These two effects, under the quasi-steady assumption, are governed by the dimensionless equations (with R/a rewritten now as R)

$$\dot{\theta} = \omega_y(R, \theta) \qquad [3.15]$$

and

$$\dot{R} = -2U_x(R, \theta). \qquad [3.16]$$

Figures 8 and 9 show the evolution of R and θ as determined by integrating [3.15] and [3.16] with a fourth order Runge–Kutta routine. The plots include the curve

$$R = 2(1 - e^2 \cos^2 \theta)^{1/2},$$

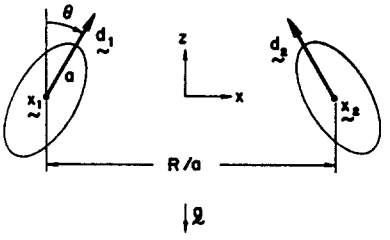

Figure 7. Mirror symmetry geometry of two inclined spheroids with their axes in a vertical plane.

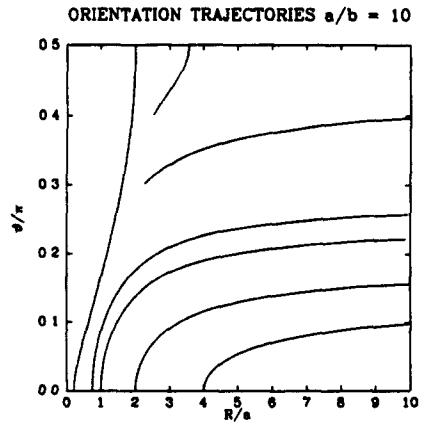

Figure 8. Evolution of orientation and separation for two spheroids, aspect ratio = 10, falling as in figure 7.

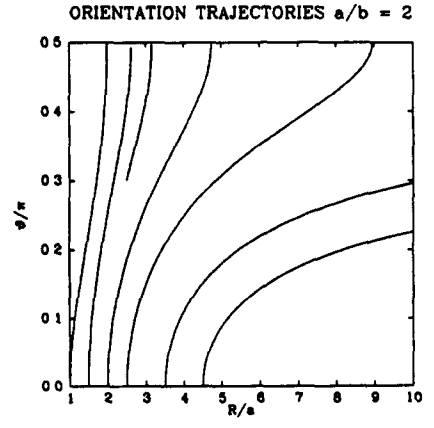

Figure 9. Evolution of orientation and separation for two spheroids, aspect ratio = 2, falling as in figure 7.

for contact between the two spheroids. Figures 10 and 11 show the corresponding trajectories of the centroid of spheroid 2 in the x–z plane.

If the orientation trajectories are followed from $\theta = 0$ (vertically oriented spheroids) and all allowed values for R, the curves in figures 8 and 9 fall into two groups, depending on the initial value of R. If R exceeds a critical value at $\theta = 0$, the particles eventually and monotonically separate and the orientations approach asymptotically a limiting value for θ

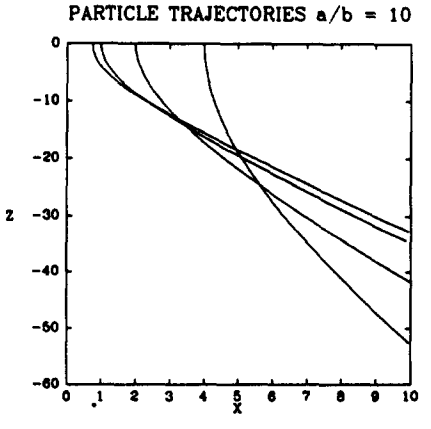

Figure 10. Trajectories for the centroid of spheroid 2 corresponding to the curves in figure 8 (aspect ratio = 10).

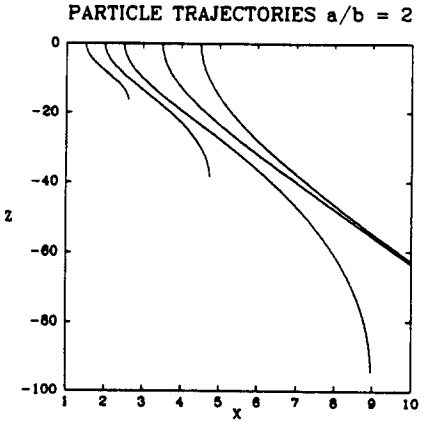

Figure 11. Trajectories for the centroid of spheroid 2 corresponding to the curves in figure 9 (aspect ratio = 2).

which is less than $\pi/2$ because at large separations, ω goes to zero. However, for initial values of R less than the critical value, the rotational motion is sufficiently large to cause the particles to rotate beyond the horizontal orientation. Thereafter, the particles drift towards each other along trajectories which are mirror images of the outward trajectories. The separatrix which starts at the critical values of R has the asymptote $\theta^{\infty} = \pi/2$ (horizontal orientation).

The asymptotic behavior at large R can be obtained by using only the leading term in ω_y and that in U_x. Equations [3.15] and [3.16] can then be integrated analytically. It is found that the trajectories approach the limiting orientation θ^{∞} as

$$R^{-1} = (1 - \alpha_1/\alpha_2)(\cos 2\theta - \cos 2\theta^{\infty})/(4e\alpha_1). \qquad [3.17]$$

The influence of the aspect ratio is seen by comparing figure 8 with 9 for aspect ratios of 10 and 2, respectively. For slender particles, the periodic trajectories must squeeze through a very narrow corridor at $\theta = 0$. As the aspect ratio is reduced, this corridor widens and the periodic trajectories become more like the straight vertical lines of the spherical case.

The preceding analysis has shown that $R(t)$ and $\theta(t)$ for the particle geometry of this subsection are either periodic or represent single encounters. Accurate calculation of the separatrix required the higher reflections, particularly at large aspect ratios.

Acknowledgements—This work was sponsored by the United States Army under Contract DAAG29-80-C-0041 and partially supported by grants from the AMOCO Foundation and the Rohm and Haas Company.

NOTATION

- a major semi-axis of spheroid.
- b minor semi-axis of spheroid.
- c distance from center to foci.
- $\mathbf{d}$ unit vector denoting orientation of spheroid axis.
- e eccentricity of the spheroid.
- $\mathbf{e}$ rate-of-strain tensor.
- $\mathbf{F}$ force exerted on the particle by the fluid.
- $\mathbf{g}$ gravitational vector.
- $\mathbf{I}$ Oseen tensor.
- R center to center separation between two spheroids.
- $\mathbf{S}$ stresslet or symmetric part of the stress dipole.
- $\mathbf{T}$ torque exerted on the particle by the fluid.
- $\mathbf{U}$ particle translational velocity.

$\mathbf{v}$ velocity.
$\mathbf{x}$ position vector.

Greek letters

α constants in the Chwang–Wu singularity solutions.
γ constants in the Chwang–Wu singularity solutions.
δ identity tensor.
ϵ alternating tensor.
θ angle defined in figure 7.
μ viscosity.
ξ vector denoting position on the spheroid axis.
σ stress tensor.
ϕ_1, ϕ_2 angles defined in figure 1.
ψ angle defined in figure 1.
ω particle angular velocity.
Ω vorticity.
Ω vorticity tensor.

Subscripts

1, 2 refers to spheroids at $\mathbf{x}_1$, $\mathbf{x}_2$.
i, j, k, l, m indices used in the Einstein summation convention.

Superscripts

(n) denotes association with the nth reflection.
∞ ambient field.

REFERENCES

BATCHELOR, G. K. 1976 Brownian diffusion of particles with hydrodynamic interaction. *J. Fluid Mech.* **74,** 1–29.

BIRD, R. B., HASSAGER, O., ARMSTRONG, R. C. & CURTISS, C. 1977 *Dynamics of Polymeric Liquids,* Vol. 2 *Kinetic Theory.* Wiley, New York.

BRENNER, H. 1972 Suspension rheology. *Progress in Heat and Mass Transfer.* Pergamon, New York, Vol. 5, pp. 89–129.

CHWANG, A. T. & WU, T. Y. 1974 Hydromechanics of low-Reynolds-number flow. Part 1. Rotation of axisymmetric bodies. *J. Fluid Mech.* **63,** 607–622.

CHWANG, A. T. & WU, T. Y. 1975 Hydromechanics of low-Reynolds-number flow. Part 2. Singularity method for Stokes flows. *J. Fluid Mech.* **67,** 787–815.

FELDERHOF, B. U. 1977 Hydrodynamic interaction between two spheres. *Physica* **89A,** 373–384.

GIESEKUS, H. 1962 Elasto-viskose Flussigkeiten, fur die in stationaren Schichtstromungen samtliche Normalspannungskomponenten verschieden grosse sind. *Rheol. Acta* **2,** 50–62.

GLENDINNING, A. B. & RUSSEL, W. B. 1982 A pairwise additive description of sedimentation and diffusion in concentrated suspensions of hard spheres. *J. Colloid Interface Sci.* **89,** 124–143.

GLUCKMAN, M. J., PFEFFER, R. & WEINBAUM, S. 1971 A new technique for treating multiparticle slow viscous flow: Axisymmetric flow past spheres and spheroids. *J. Fluid Mech.* **50,** 705–740.

GOLDMAN, A. J., COX, R. G. & BRENNER, H. 1966 The slow motion of two identical arbitrarily oriented spheres through a viscous fluid. *Chem. Eng. Sci.* **21,** 1151–1170.

HAPPEL, J. & BRENNER, H. 1965 *Low Reynolds number hydrodynamics.* Prentice-Hall, Princeton.

HINCH, E. J. & LEAL, L. G. 1972 The effect of Brownian motion on the rheological properties of a suspension of non-spherical particles. *J. Fluid Mech.* **52,** 683–712.

JEFFREY, D. J. & ONISHI, Y. 1984 Calculation of the resistance and mobility functions for two unequal rigid spheres in low-Reynolds-number flow. *J. Fluid Mech.* **139,** 261–290.

KIM, S. 1983 Ph.D. dissertation. Princeton University.

KIM, S. 1985 A note on Faxen laws for nonspherical particles. *Int. J. Multiphase Flow* **11,** 713–719.

LIAO, W. & KRUEGER, D. A. 1980 Multipole expansion calculation of slow viscous flow about spheroids of different sizes. *J. Fluid Mech.* **96,** 223–241.

ROTNE, J. & PRAGER S. 1969 Variational treatment of hydrodynamic interaction in polymers. *J. Chem. Phys.* **50,** 4831–4837.

STIMSON, M. & JEFFREY, G. B. 1926 The motion of two spheres in a viscous fluid. *Proc. Roy. Soc. London. Ser. A* **111,** 110–116.

WAKIYA, S. 1965 Mutual interaction of two spheroids sedimenting in a viscous fluid. *J. Phys. Soc. Jpn.* **20,** 1502–1514.

YAMAKAWA, H. 1970 Transport properties of polymer chains in dilute solution: Hydrodynamic interaction. *J. Chem. Phys.* **53,** 436–443.

APPENDIX

The numerical convergence with each additional reflection is shown in the following tables. The geometry is as in figure 7 and the velocities have been scaled with U^∞, the sedimentation velocity of an isolated, vertically oriented spheroid.

Table 1. Inclined spheroids: Effect of successive reflections

	Aspect ratio = 1 and R/a = 3.0		
	U_{1x}/U^∞	U_{1z}/U^∞	$\omega_{1y}a/U^\infty$
zeroth reflection	0.00000	1.00000	0.00000
with first reflection	0.00000	1.26852	0.08333
with second reflection	0.00000	1.26852	0.08333
exact solution	0.00000	1.26680	0.08178
	Aspect ratio = 2, θ = 0 and R/a = 1.5		
	U_{1x}/U^∞	U_{1z}/U^∞	$\omega_{1y}a/U^\infty$
zeroth reflection	0.00000	1.00000	0.00000
with first reflection	0.00000	1.32692	0.12419
with second reflection	0.00000	1.32886	0.12457
	Aspect ratio = 2, $\theta = 0.3\pi$ and R/a = 2		
	U_{1x}/U^∞	U_{1z}/U^∞	$\omega_{1y}a/U^\infty$
zeroth reflection	0.06033	0.91697	0.00000
with first reflection	0.06033	1.18429	0.13897
with second reflection	0.05296	1.18259	0.14073
	Aspect ratio = 10, θ = 0, and R/a = 0.7		
	U_{1x}/U^∞	U_{1z}/U^∞	$\omega_{1y}a/U^\infty$
zeroth reflection	0.00000	1.00000	0.00000
with first reflection	0.00000	1.28195	0.07562
with second reflection	0.00000	1.28785	0.06962
	Aspect ratio = 10, $\theta = 0.3\pi$ and R/a = 2		
	U_{1x}/U^∞	U_{1z}/U^∞	$\omega_{1y}a/U^\infty$
zeroth reflection	0.14531	0.80000	0.00000
with first reflection	0.14531	0.91759	0.06406
with second reflection	0.14238	0.91754	0.06416

Table 2. Comparison with the boundary collocation solution of Gluckman *et al.* (1971) for axisymmetric uniform streaming. λ is the spheroidal drag divided by the drag on a sphere with the same cross-sectional area

R/a	Method of reflections	Collocation
	Aspect ratio = 2	
2	0.8485	0.8442
4	0.9811	0.9812
6	1.0458	1.0458
	Aspect ratio = 5	
2	1.3673	1.3700
4	1.5675	1.5675
6	1.6364	1.6364